THE ANALYSIS OF SURGE

by

Ross H. Sentz

Senior Engineer

Union Carbide Corporation

Linde Division

Tonawanda, New York

Ross H. Sentz is senior engineer in the Mechanical Equipment Group of the Linde Division of Union Carbide Corporation, where he is responsible for the field vibration analysis of rotating equipment and performance evaluation of turbomachinery.

Mr. Sentz has had twelve years' experience in turbomachinery, primarily in the areas of analytical stress, vibration studies, and field vibration testing. He holds a B.S. degree in Engineering Mechanics from Lehigh University and a M.S. degree in Mechanical Engineering from Union College.

As a member of the adjunct faculty of Union College in Schenectady, New York, he has taught courses in thermodynamics, convection heat transfer, and continuum mechanics.

ABSTRACT

Recently, considerable attention has been given to the phenomenon of surge in compressors and pumps. Typically, the model under study is a Helmholtz resonator and driver where the flow in the delivery duct to the resonator is assumed incompressible. The objective of this analytical study is to extend this model to one more applicable to field situations and to discuss the impact of some of the added effects. In particular, these effects are: heat transfer in the exhaust chamber, the action of the momentum flux on the fluid boundaries in the duct and the compressibility of the gas in the delivery duct. The equations retain their nonlinear character and are solved numerically. The instability condition is reported and discussed.

INTRODUCTION

In recent years considerable attention has been given to the phenomenon of surge in compressors and pumps [1,2,3,4,5]. Typically, the model under study is a Helmholtz resonator and a driver where the flow in the delivery duct to the resonator is assumed incompressible. The objective of this analytical study is to extend this model to one more applicable to field situations (Figure 1) and to discuss the impact of some of the added effects. The assumptions made here are:

1. Heat transfer occurs in the exhaust chamber.
2. The action of the momentum flux on the fluid boundaries in the delivery duct is retained.
3. The flow in the delivery duct is compressible and isothermal.
4. The time rate of change of the mass of gas in the delivery duct is negligible.
5. The compressor responds quasi-steadily to changes in flow.

The equations are solved numerically with the nonlinearities retained.

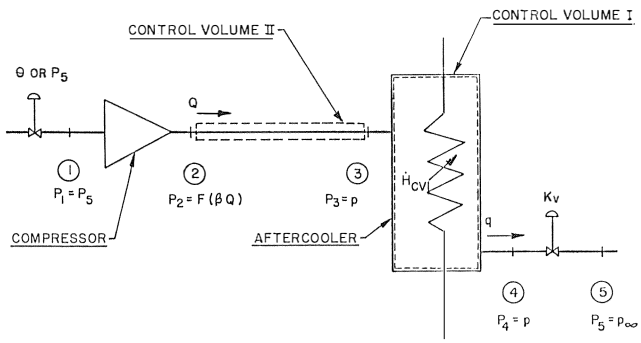

Figure 1. System Schematic.

DIFFERENTIAL EQUATIONS OF THE SYSTEM

The compressor characteristic, F (βQ), is normally one of two forms depending on the means of control. If the compressor is suction throttled, F (βQ) is a one parameter family of curves with the identifying parameter being suction pressure, P_s, which represents the degree of freedom of control. On the other hand, the flow may be controlled by variable inlet guide vanes. In this case the angle setting of the guide vanes, Θ, is the degree of freedom of control.

The system is provided with a throttle downstream of the after-cooler. We assume the pressure drop across the throttle is of the form

$$p_4 - p_5 = K_v Q_4^2 \qquad (1)$$

For this valve K_v is the degree of freedom of control. The quantities K_v, P_s, and Θ are regarded as arbitrary, within practical limits, in the analysis below.

If we write the mass and energy balances for control volume I, we get, after some simplification,

$$\frac{dp}{dt} = \frac{k}{V}[F(\beta Q)Q - pq] - \frac{778}{144}\frac{(k-1)}{V}\dot{H}_{CVI} \quad . \qquad (2)$$

The details of this calculation are given in the Appendix.

Denoting the pressure downstream of the throttle valve as p_0, the flow q is given by

$$p_4 - p_5 = p - p_\infty = K_v q^2 \qquad (3)$$

Using equation (3) to eliminate q in equation (2), we have

$$\frac{dp}{dt} = \frac{k}{V}\left[F(\beta Q)Q - p\sqrt{\frac{p-p_\infty}{K_v}} - \frac{778}{144}\frac{(k-1)}{k}\dot{H}_{CVI}\right] . \quad (4)$$

The balance of momentum for control volume II yields after the calculations given in the Appendix,

$$\frac{d}{dt}[F(\beta Q)Q] = \frac{60[F(\beta Q)-p]}{L}\left[60g_cART_D - \frac{F(\beta Q)Q^2}{60Ap}\right] \quad (5)$$

where we have converted the units of time from seconds to minutes.

Equations (4) and (5) constitute two simultaneous nonlinear ordinary differential equations for the volumetric flow Q and the pressure in the after-cooler p. In this study, the equations will be solved numerically as an initial value problem. A point of stable operation is selected as the initial point and the system is throttled back into surge. It is important to emphasize that the compressor characteristic must be fitted with care in order not to artificially introduce a singularity in the domain of definition. Specifically, $F'(\beta Q) + F$ must not vanish at any flow where we wish to calculate the next time step.

EQUILIBRIUM AND INSTABILITY

Define

$$f(Q,p,K_v) = \frac{k}{V}\left[F(\beta Q)Q - p\sqrt{\frac{p-p_\infty}{K_v}}\right] - \frac{778}{144}\frac{(k-1)}{V}\dot{H}_{CVI} \quad (6)$$

and

$$g(Q,p) = \frac{60}{L}\left[F(\beta Q)-p\right]\left[60g_cART_D - \frac{F(\beta Q)Q^2}{60Ap}\right]. \quad (7)$$

Equilibrium occurs under the condition that both $f(Q,p,K_v)$ and $g(Q,p)$ vanish simultaneously so that Q and p vanish for all t. So equilibrium occurs at a point (Q_0,p_0) such that

$$f(Q_0,p_0,K_v) = 0 \quad (8)$$

and

$$g(Q_0,p_0) = 0 \quad . \quad (9)$$

As we might expect, this occurs in equation (9) when

$$p_0 = F(\beta Q_0) \quad (10)$$

and in equation (8) when we have adjusted the valve setting, i.e., selected a value of K_v, such that equation (8) is satisfied for

$$f(Q_0, F(\beta Q_0), K_v) = 0 \quad . \quad (11)$$

All operating points of practical interest satisfy these steady flow conditions. There exist, however, some points (Q_0,p_0) that are not stable. Since K_v is a free parameter, clearly we can throttle back over a considerable range of flow. Should we select a K_v setting corresponding to one of these unstable equilibrium points, the system goes into surge which exhibits itself as a limit cycle in the Q-p plane. According to references [6] and [7], the unstable equilibrium points satisfy the relation

$$\left.\frac{\partial f}{\partial p}\right|_{Q_0,p_0} + \left.\frac{\partial g}{\partial Q}\right|_{Q_0,p_0} > 0$$

For the equilibrium conditions described by equations (10) and (11), the condition for instability is

$$60F'(\beta Q_0)\beta\left[60g_cART_D - \frac{Q_0^2}{60A}\right] > \frac{k}{V}\left[\sqrt{\frac{p-p_\infty}{K_v}} + \frac{p}{2\sqrt{K_v(p-p_\infty)}}\right]. \quad (12)$$

Inspection of the inequality (12) reveals that a necessary condition for surge is that the slope of the characteristic be positive for surge to occur if

$$\sqrt{3600g_cRT_D} > \frac{Q_0}{A} \quad , \quad (13)$$

which is normally the case. The reason for this is that sonic velocity in the delivery duct is given by

$$\left(\frac{Q}{A}\right)_{sonic} = \sqrt{3600kg_cRT_D} \quad \text{fpm.} \quad (14)$$

So the lefthand side of equation (13) is less than sonic velocity by a factor $1/\sqrt{k}$. Normally the flow velocities in the delivery duct are well under sonic velocity in the operating range and during surge since the compressor itself would be in choke long before its downstream delivery duct.

In passing it should be pointed out that there exists another set of stable equilibrium points satisfying

$$F(\beta Q_0)Q_0^2/60Ap_0 = 60g_cART_D$$

and equation (11). These points, however, are physically extraneous. For the example discussed below, this would imply $p_0 < p_\infty$, which cannot occur.

The role of the system parameters in the determination of the instability threshold of flow is revealed by inspection of the inequality (12). For example, increasing the volume V of the aftercooler tends to reduce the practical operating range by raising the instability threshold flow on its lower end. There is a definite limit, however, to the extent of this effect. As V gets very large, the instability threshold approaches the flow where the compressor characteristic peaks out since $F'(\beta Q_0)$ approaches zero. Lengthening the delivery duct tends to widen the operation range by lowering the instability threshold. Again, since velocities are well below sonic in the duct, increasing the cross-sectional area of the delivery duct lowers the threshold of instability, thus increasing the operational range. Because of practical limitations on the range of selection of V, L and A, it is the shape of the compressor characteristic itself, and more specifically, its slope $F'(\beta Q)$, that overwhelmingly dominates the calculation of the threshold of instability. In fact, the threshold of instability will differ very little from the Q_0 satisfying

$$F'(\beta Q_0) = 0 \text{ and } F''(\beta Q_0) < 0 \quad ,$$

as was observed in reference [8].

ILLUSTRATIVE EXAMPLE

Consider a centrifugal compressor having the characteristic indicated by the dashed line in Figure 2. The parameters for the system shown in Figure 1 are as follows:

Dimensions of the delivery duct:

Cross-sectional area A: 1.4 ft.^{2}

Length: 10 ft.

Volume of aftercooler V: 30.4 ft.^{3}
Heat transfer rate in aftercooler $\dot{H}_{CVI}$: 7×10^6 Btu/hr.
Compressor suction P_s: 79.0 psia
Compressor discharge temperature T_D: 184°F

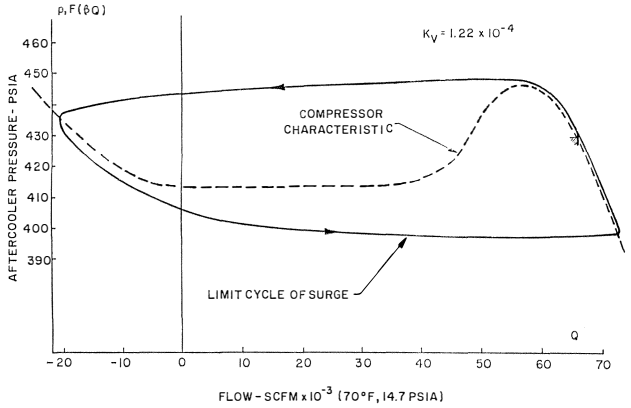

Figure 2. The Surge Limit Cycle in the p-Q Plane.

With the system running at the design point p = 430 psia and Q = 66,000 scfm and blowing off to atmosphere, we throttle back the discharge valve to give us a value of $K_v = 1.22 \times 10^{-4}$ lbf/in^2 (scfm)^2 which we know by relation (12) will produce a surge instability in the system. The aftercooler pressure p responds by rising slightly ahead of the discharge pressure of the compressor indicated by the dashed line in Figure 2. Inspection of equation (11) indicates that the sign of $(F(\beta Q) - p)$ controls whether Q increases or decreases with time, as we might expect. After the aftercooler pressure exceeds the maximum pressure the compressor can deliver, the flow Q begins dropping very rapidly and even reverses in this case. The flow does not increase again until the discharge pressure exceeds the aftercooler pressure, i.e., until the phase plane $(p - Q)$ trajectory crosses the characteristic. The aftercooler pressure drops more rapidly as the flow increases and eventually flows positively again. This persists until the aftercooler pressure again exceeds the discharge pressure. Then p rises, skirts past the design point at a slightly higher pressure at the design flow. The system then repeats a similar pattern of flow oscillation and is virtually into its limit cycle in the second oscillation.

Inspection of the time domain response in Figure 3 indicates a fluttering of discharge pressure in spurts as the flow rapidly descends into its reversal and recovers. We can also see the mean flow is positive since the negative areas below the flow axis obviously cannot balance out the positive ones above the axis. Figure 4 shows the time history of a transition between two stable operation points from p = 430 psia and Q = 66,000 scfm to p = 421.9 psia. The discharge pressure and the aftercooler pressure are so close they would not be able to be distinguished on a phase plane $(p - Q)$ plot.

CONCLUSIONS

One practical conclusion to be drawn from the illustrative example is that the maximum aftercooler pressure only slightly exceeds the local maximum discharge pressure where $F'(\beta Q) = 0$ during the surge transient.

Inspection of equation (5) for the given numerical values and characteristic indicates that the effect of the momentum

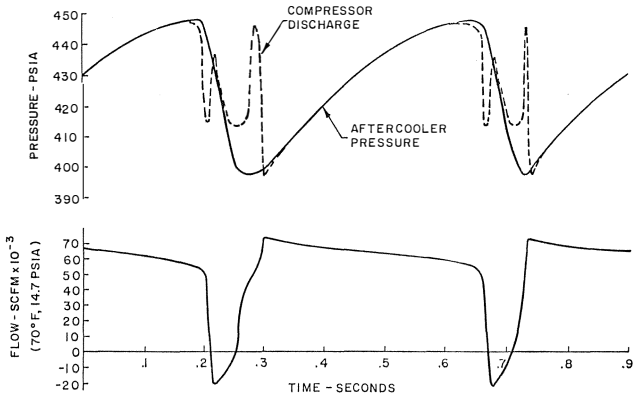

Figure 3. Time History of the Surge.

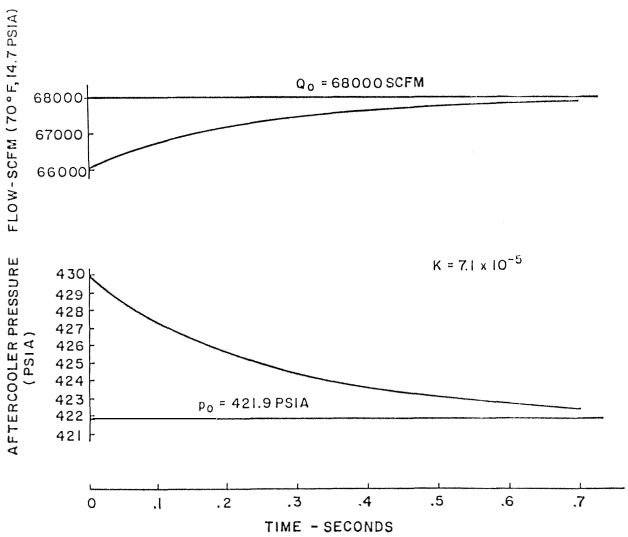

Figure 4. Transition Between Two Stable Operating Points.

flux term quantitatively affects the results by about 7% in the right hand corner of the limit cycle in Figure 2 down to 0% where the flow reverses. Qualitatively, it does not affect the results at all. One would be on firm ground neglecting it.

The heat transfer functions to bias the system against a pressure increase with respect to time. The aftercooler pressure decreases more rapidly than it increases as Q is varied. One can reinterpret this system as a gas turbine compressor by reversing this effect with the sign change of $\dot{H}_{CVI}$. The discharge chamber, then, is visualized as the combustion chamber where heat is added rather than removed. In this case, the limit cycle would hug the characteristic closer on the underside and rise higher with more curvature on the topside.

APPENDIX A: *DIFFERENTIAL EQUATIONS OF THE SYSTEM*

The system is provided with a throttle downstream of the aftercooler. We assume the pressure drop across the throttle is of the form

$$p_4 - p_5 = K_v Q_4^2 \qquad \text{(A-1)}$$

For this valve K_v is the degree of freedom of control. The quantities K_v, P_s and Θ are regarded as arbitrary, within practical limits, in the analysis below.

Consider control volume I around the aftercooler. The balance of mass is

$$\frac{dM}{dt} = \dot{m}_3 - \dot{m}_4 \qquad \text{(A-2)}$$

where

$$M(t) = \int_v \rho dV \qquad \text{(A-3)}$$

is the mass of the gas inside the aftercooler. An energy balance yields

$$-\dot{H}_{CVI} + \dot{m}_3 h_3 = \dot{m}_4 h_4 + \frac{dE_{CVI}}{dt} \qquad \text{(A-4)}$$

where

$$E_{CVI}(t) = \int_v \rho u dV \qquad \text{(A-5)}$$

is the total energy of the gas in the aftercooler.

Neglecting any time rate of change of the mass of the gas in the delivery duct between stations 2 and 3 (Figure 1), we have,

$$\dot{m}_3 = \dot{m}_4 = \rho_2 Q \qquad \text{(A-6)}$$

and

$$\dot{m}_4 = \rho_4 Q_4 = \rho_4 q \quad . \qquad \text{(A-7)}$$

In the aftercooler we have an approximately isobaric process. So

$$p_3 = p_4 = p \quad . \qquad \text{(A-8)}$$

Since

$$p = \rho R T \quad , \qquad \text{(A-9)}$$

equation (A-8) implies

$$\rho_3 T_3 = \rho T_4 = \frac{p}{R} \quad . \qquad \text{(A-10)}$$

By definition of the enthalpy per unit mass, we have

$$h = u + \frac{p}{\rho} \qquad \text{(A-11)}$$

and for an ideal gas with constant specific heats we have

$$u = C_v(T - T_{ref}) \qquad \text{(A-12)}$$

where T_{ref} is the reference temperature appropriate to C_v. Substituting equation (A-12) into equation (A-5), we get

$$E_{CVI}(t) = \int_v \rho C_v (T - T_{ref}) dV \quad . \qquad \text{(A-13)}$$

Assuming C_v constant and using equations (A-5) and (A-9) in equation (A-13), we get

$$E_{CVI}(t) = \frac{C_v V p}{R} - C_v T_{ref} M(t) \quad , \qquad \text{(A-14)}$$

where V is the volume of the aftercooler.

Substituting equations (A-6), (A-7), (A-11) and (A-14) into equation (A-2) yields

$$-\dot{H}_{CVI} + \rho_2 Q C_v (T_3 - T_{ref}) + \rho_2 Q \frac{p}{\rho_3}$$

$$= \rho_4 q C_v (T_4 - T_{ref}) + qp + \frac{C_v V}{R} \frac{dp}{dt} - C_v T_{ref} \frac{dM}{dt} \quad . \qquad \text{(A-15)}$$

Rearranging and using equations (A-2), (A-6) and (A-7), the terms having T_{ref} cancel out.

Simplifying with equation (A-9), equation (A-15) becomes

$$-\dot{H}_{CVI} + \rho_2 Q C_v T_2 + \rho_2 Q \frac{p}{\rho_4} = \frac{C_v}{R} pq + pq + \frac{C_v V}{R} \frac{dp}{dt} \quad . \qquad \text{(A-16)}$$

Assuming no temperature drop along the delivery duct, we have

$$\frac{p_3}{\rho_3} = \frac{p_2}{\rho_2} = \frac{F(\beta Q)}{\rho_2} \quad \text{and} \quad T_3 = T_2 \quad . \qquad \text{(A-17)}$$

Simplifying equation (A-16) with equations (A-17) and (A-9) and using the relations

$$C_p - C_v = R \quad \text{and} \quad k = C_p / C_v \quad ,$$

equation (A-16) reduces to

$$\frac{dp}{dt} = \frac{k}{V}(F(\beta Q)Q - pq) - \frac{778}{144}\frac{(k-1)}{V}\dot{H}_{CVI} \qquad \text{(A-18)}$$

where we have selected the following units: $F(\beta Q)$ and p in psia, Q and q in cfm, V in ft^3, $\dot{H}_{CVI}$ in Btu/min and t in minutes.

Denoting the pressure downstream of the throttle valve as p_0, the flow q is given by

$$p_4 - p_5 = p - p_\infty = K_v q^2 \quad . \qquad \text{(A-19)}$$

Solving equation (A-19) for $p \geq p_\infty$ we get

$$q(p) = \sqrt{\frac{p - p_\infty}{K_v}} \quad . \qquad \text{(A-20)}$$

Using equation (A-20) to eliminate q in equation (A-18), we have

$$\frac{dp}{dt} = \frac{k}{V}\left[F(\beta Q)Q - p\sqrt{\frac{p - p_\infty}{K_v}} - \frac{778}{144}\frac{(k-1)}{k}\dot{H}_{CVII}\right] \qquad \text{(A-21)}$$

Turning now to control volume II enclosing the delivery duct, we write the balance of momentum. The time rate of change of momentum will have two parts:

1. the time rate of change of momentum within the control volume, and
2. the rate of change of momentum flux on the boundaries.

Thus:

$$\text{Momentum in CVII} = \frac{1}{g_c}\int_v \rho(x) v_x(x) dV \quad . \qquad \text{(A-22)}$$

Let $\tilde{Q}(x)$ be the volumetric flow in cfm at location x between stations 2 and 3 (Figure 1), then we have

$$v_x(x) = \frac{\tilde{Q}(x)}{60A} \text{ fps}$$

and

$$\rho(x)v_x(x) = \rho(x)\frac{\tilde{Q}(x)}{60A} \tag{A-23}$$

where A is the cross-sectional area of the duct in square feet. Neglecting the time rate of change of the mass of gas in the delivery duct, we have

$$\rho(x)\tilde{Q}(x) = \rho_3 Q_3 = \rho_2 Q \tag{A-24}$$

and

$$\rho_2 = \frac{p_2}{RT_2} = \frac{144F(\beta Q)}{RT_D} \text{ lbm/ft}^3 \tag{A-25}$$

where R is in lbf-ft/lbm-°R and T_D is in degrees Rankine (°R). Using equations (A-23), (A-24) and (A-25) in equation (A-22), we get

$$\int_v \rho(x)v_x(x)dV = \frac{144}{60}\frac{F(\beta Q)QL}{RT_D} \tag{A-26}$$

where L is the length of the delivery duct in feet. So the time rate of change of momentum within the control volume is given by

$$\frac{1}{g_c}\frac{d}{dt}\left[\int_v \rho v_x dV\right] = \frac{144L}{60g_c RT_D}\frac{d}{dt}(F(\beta Q)Q) \quad . \tag{A-27}$$

The rate of change of momentum flux at the boundaries of the control volume can be shown by elementary methods to be

$$\frac{1}{g_c}\oint \rho v_x(\vec{v}\cdot\hat{n})dS = \frac{1}{3600g_c A}(\rho_3 Q_3^2 - \rho_2 Q^2) \quad .$$

Using equations (A-17), (A-24) and (A-25), this reduces to

$$\frac{1}{g_c}\oint \rho v_x(\vec{v}\cdot\hat{n})dS = \frac{144F(\beta Q)Q^2}{3600g_c ART_D}\left(\frac{F(\beta Q)-p}{p}\right) \quad . \tag{A-28}$$

The action of the pressure on the boundary of the control volume is

$$-\oint p n_x dS = -144(p - F(\beta Q))A \quad . \tag{A-29}$$

The balance of momentum is

$$\frac{1}{g_c}\frac{d}{dt}\left[\int_v \rho v_x dV\right] + \frac{1}{g_c}\oint \rho v_x(\vec{v}\cdot\hat{n})dS = -\oint p n_x dS \tag{A-30}$$

where viscous friction has been neglected. Using equations (A-27), (A-28) and (A-29) in equation (A-30), we get the remaining equation for the system

$$\frac{d}{dt}[F(\beta Q)Q] = \frac{60(F(\beta Q)-p)}{L}\left[60g_c ART_D - \frac{F(\beta Q)Q^2}{60Ap}\right] . \tag{A-31}$$

REFERENCES

1. Emmons, H. W., Pearson, C. E., and Grant, H. P., "Compressor Surge and Stall Propagation," Trans. ASME, Vol. 77, April 1955, pp. 455-469.
2. Dean, R. C., Jr. and Young, L. R., "The Time Domain of Centrifugal Compressor and Pump Stability and Surge," *Journal of Fluids Engineering*, Trans. ASME, March 1977, pp. 53-63.
3. Greitzer, E. M., "Surge and Rotating Stall in Axial Flow Compressors — Part I: Theoretical Compression System Model, and Part II: Experimental Results and Comparison with Theory," *Journal of Engineering for Power*, Trans. ASME, April 1976, pp. 190-217.
4. Gyarmathy, G. "Nonlinear Analysis of Surge Cycles," *Journal of Fluids Engineering*, Trans. ASME, March 1977.
5. Rothe, P. H. and Runstadler, P. W., Jr., "First Order Pump Surge Behaviour," *Journal of Fluids Engineering*, Trans. ASME, Vol. 100, No. 4, Dec. 1978, p. 459.
6. Davis, H. T., *Introduction to Nonlinear Differential and Integral Equations* (New York: Dover Publications).
7. Bellman, R. C., *Stability Theory of Differential Equations* (New York: Dover Publications).
8. Stodola, A., *Steam and Gas Turbines* (New York: McGraw-Hill Book Company, 1927).